golden light
publishing®

RESEARCH ARTICLE

Advanced frequency of thick FGM cylindrical shells with fully homogeneous equation

CC Hong[1*]

[1] Hsiuping University of Science and Technology, Department of Mechanical Engineering, Taiwan, ROC

Abstract

The effects of shear deformation theory and improved shear correction factors on the advanced computation of frequencies by using the fully homogeneous equation for thick functionally graded material (FGM) circular cylindrical shells are studied. It is quite reasonable to consider the extra advanced effect of third-order shear deformation theory (TSDT) of displacements on the varied shear correction coefficient. The values of advanced nonlinear shear correction coefficient are usually functions of the nonlinear coefficient term in TSDT, power-law exponent parameter, and environment temperature. The main achievements in the nonlinear case of displacements and with the varied value of shear correction coefficients, the non-dimensional fundamental frequencies are estimated, investigated, and compared with the values in the linear case. This paper aims to study the fundamental frequencies of very thick FGM cylindrical shells under the advanced effects of shear deformation theory and improved shear correction factors.

1. Introduction

Usually, the shear deformation theory of displacements need not be considered in the thin shell analyses, and it is usually considered for the thick shell analyses. To include the varied effect of stress across the thickness direction for the thick shells, it would be usually to consider the shear deformation theory of displacements in the study. For the moderate thick (e.g. aspect ratio equal to 10) shell analyses, first-order shear deformation theory (FSDT) is usually used. For the very thick (e.g. aspect ratio equal to 5) shell analyses, third-order shear deformation theory (TSDT) is usually used. The originality of this paper is to provide the difference from the studies in the published literature. This paper provides both the shear deformation theory and improved shear correction factors in the effect of frequencies, especially for the very thick plates and shells, in the following published literature were seldom investigations of the improved and advanced studies. Several investigations of the improved shear deformation theory of displacements on the thick beams, plates, and shells. Birman and Bert [1] presented several models of shear correction factors in multi-layer sandwich structures. Okumus [2] presented an analysis of shear correction factors for a thermoplastic cantilever beam. Daouadji et al. [3] presented a new higher-order shear deformation theory (HSDT) of displacements with no shear correction factor for the static behavior of functionally graded material (FGM) plates. Xiang et al. [4] presented the natural frequencies of FGM plates resting on elastic foundations by using the nth-order shear

deformation theory of displacements with no shear correction factor. Lim [5] presented the improved shear correction factors for the deflection of simply supported very thick rectangular auxetic plates, without considering the effect of FSDT and TSDT of displacements for the natural frequency. Bouhlali et al. [6] presented the nonlinear thermo-elastic analysis of thick FGM plates without considering the effect of shear correction factors. Ghamkhar et al. [7] presented the vibration frequency analysis of three-layered FGM cylinder shells with the numerical method by considering the axial and circumferential wave numbers of mode shapes. Nguyen et al [8] presented the refined FSDT of displacements and no shear correction factor to investigate the free vibration of FGM plates. In 2020, Ganczarski and Szubartowski [9] presented the thermo-mechanical analysis for thick-walled FGM cylinders including thermal barrier coating by using a special graded finite element method. Vuong and Duc [10] presented the nonlinear vibration of moderately thick FGM shells resting on elastic foundations by using the TSDT of displacements.

Some contact problems of functionally graded materials (FGMs) were also presented. Yaylaci et al. [11] presented the contact mechanics of FGMs in the rigid foundation and pressed punch, the body force was also included in the analysis of the finite element method (FEM). Adiyaman et al. [12] presented the contact problems of the FGM beam under the distributed pressure loads, the body force was also included in the analysis. Yaylaci et al. [13] presented the frequencies and buckling of the FGM beam by using the FEM and multilayer perceptron (MLP). Adiyaman et al. [14] also presented the contact problems of FGM beams for studying the behavior of materials. Turan et al. [15] presented the frequencies and buckling of FGM porous beams by using the FSDT, FEM, and artificial neural network (ANN) methods. There were seldom investigations of the improved shear correction factors on the very thick plates and shells.

Mode shape values of non-dimensional frequency parameters are decreasing firstly vs. circumferential nodes in the linear case of displacements and with a constant value of shear correction coefficient. There were several investigations of the improved shear correction factors on the thick shells. Hong [16] presented the preliminary studies in free vibration frequency of thick FGM spherical shells with simply homogeneous equations by using TSDT of displacements and the linear calculation of varied shear correction coefficients. Hong [17] presented the preliminary studies in free vibration frequency of thick FGM circular cylindrical shells without considering the effects of the nonlinear coefficient TSDT term on the calculation of varied shear correction coefficients. Hong [18] presented the basic studies of the varied shear correction and FSDT effects on the vibration frequency of thick FGM circular cylindrical shells in unsteady supersonic flow. Hong [19] presented the basic studies in thermal vibration of magnetostrictive FGM shells by considering the linear FSDT of displacements and varied effects of the shear correction coefficient. This paper aims to study the frequencies of very thick FGM cylindrical shells under the advanced effects of shear deformation theory and improved shear correction factors. In the advanced studies for the vibration frequency of thick FGM circular cylindrical shells with the fully homogeneous equation, it is interesting to consider the simultaneous three effects of the TSDT of displacements, the nonlinear shear correction coefficient of transverse shear force and the two directions of mode shapes. To obtain the results of natural frequencies (ω_{mn}) in which subscripts m and n are the mode shapes in x and y directions for the advanced studies of thick FGM circular cylindrical shells. The innovation of this topic is to consider two advanced effects of nonlinear shear correction coefficient and TSDT on the thick FGM circular cylindrical shells. The application of this topic in the future might be applied to the field of missile engines.

2. The formulation for the advanced nonlinear k_α

Time-dependent nonlinear displacements u, v, and w at any point (x, θ, z) of thick FGM cylindrical shells are assumed in the nonlinear coefficient c_1 term of TSDT equations as follows, based on the semi-analytical studies of laminated plates by Lee et al. [20]

$$u = u_0(x,\theta,t) + z\phi_x(x,\theta,t) - c_1 z^3 \left(\phi_x + \frac{\partial w}{\partial x}\right)$$

$$v = v_0(x,\theta,t) + z\phi_\theta(x,\theta,t) - c_1 z^3 \left(\phi_\theta + \frac{\partial w}{R\partial\theta}\right) \tag{1}$$

$$w = w(x,\theta,t)$$

where u_0 and v_0 are the tangential displacements in the in-surface coordinates x and θ axes direction, respectively. w is the transverse displacement in the out-of-surface coordinates z axis direction of the middle plane of shells. ϕ_x and ϕ_θ are the shear rotations. R is the middle-surface radius at any point (x,θ,z) of the FGM cylindrical shells that are illustrated in Fig. 1 with the thickness h_1 of FGM material 1 and thickness h_2 of FGM material 2, respectively in the thickness direction of the cylindrical coordinate systems. t is the time. The coefficient for $c_1 = 4/(3h^{*2})$ is given in the TSDT approach, in which h^* is the thickness of FGM cylindrical shells.

The normal stresses (σ_x and σ_y) and the shear stresses ($\sigma_{x\theta}$, σ_θ and σ_{xz}) of the thick FGM circular cylindrical shells under temperature difference ΔT for the kth constituent material are assumed in the following equations by Whitney [21].

$$\begin{Bmatrix} \sigma_x \\ \sigma_\theta \\ \sigma_{x\theta} \end{Bmatrix}_{(k)} = \begin{bmatrix} \bar{Q}_{11} & \bar{Q}_{12} & \bar{Q}_{16} \\ \bar{Q}_{12} & \bar{Q}_{22} & \bar{Q}_{26} \\ \bar{Q}_{16} & \bar{Q}_{26} & \bar{Q}_{66} \end{bmatrix}_{(k)} \begin{Bmatrix} \varepsilon_x - \alpha_x \Delta T \\ \varepsilon_\theta - \alpha_\theta \Delta T \\ \varepsilon_{x\theta} - \alpha_{x\theta} \Delta T \end{Bmatrix}_{(k)}$$

$$\begin{Bmatrix} \sigma_{\theta z} \\ \sigma_{xz} \end{Bmatrix}_{(k)} = \begin{bmatrix} \bar{Q}_{44} & \bar{Q}_{45} \\ \bar{Q}_{45} & \bar{Q}_{55} \end{bmatrix}_{(k)} \begin{Bmatrix} \varepsilon_{\theta z} \\ \varepsilon_{xz} \end{Bmatrix}_{(k)} \tag{2}$$

where α_x and α_θ are the coefficients of thermal expansion, $\alpha_{x\theta}$ is the coefficient of thermal shear, $\bar{Q}_{ij}$ is the transformed reduced stiffness of FGM shells, in which $\bar{Q}_{ij} = \bar{Q}_{i^s j^s}$ for subscripts $i^s, j^s = 1,2,6$ and $\bar{Q}_{ij} = \bar{Q}_{i^* j^*}$ for subscripts $i^*, j^* = 4,5$ and ε_x, ε_θ, $\varepsilon_{x\theta}$ are in-plane strains, not negligible $\varepsilon_{x\theta}$ and ε_{xz} are shear strains.
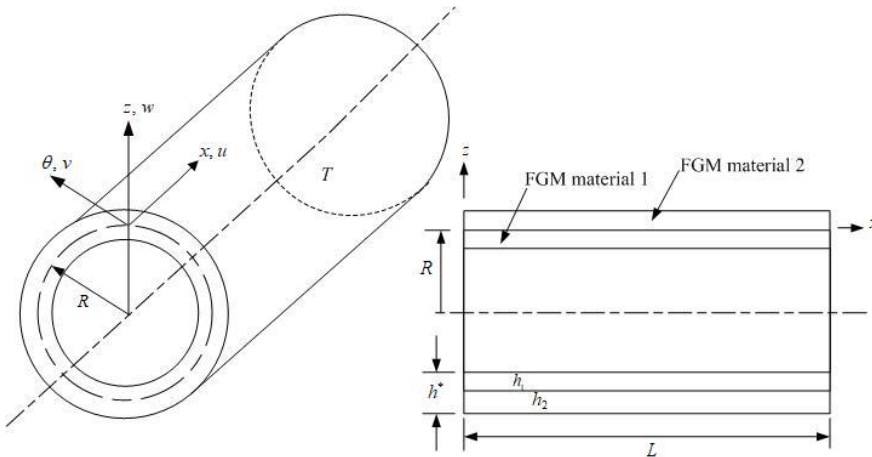

Fig. 1. Two-material thick FGM circular cylindrical shell under thermal environment T

Simpler forms of $\bar{Q}_{i^s j^s}$ and $\bar{Q}_{i^* j^*}$ for FGM cylindrical shells with z/R terms cannot be neglected are used and assumed by Sepiani et al. [22] and Hong [19] as follows:

$$\bar{Q}_{11} = \bar{Q}_{22} = \frac{E_{fgm}}{1 - \nu_{fgm}^2}$$

$$\bar{Q}_{12} = \bar{Q}_{21} = \frac{\nu_{fgm} E_{fgm}}{(1 + z/R)(1 - \nu_{fgm}^2)}$$

$$\bar{Q}_{44} = \frac{E_{fgm}}{2(1 + \nu_{fgm})} \tag{3}$$

$$\bar{Q}_{55} = \bar{Q}_{66} = \frac{E_{fgm}}{2(1 + z/R)(1 + \nu_{fgm})}$$

$$\bar{Q}_{16} = \bar{Q}_{26} = \bar{Q}_{45} = 0$$

in which $\nu_{fgm} = \frac{\nu_1 + \nu_2}{2}$ is the Poisson's ratios of the FGM cylindrical shells. $E_{fgm} = (E_2 - E_1)(\frac{z + h^*/2}{h^*})^{R_n} + E_1$ is the Young's modulus of the FGM cylindrical shells. R_n is the power-law exponent parameter E_1. and E_2 are the Young's modulus. ν_1 and ν_2 are the Poisson's ratios of the FGM constituent material 1 and 2, respectively. The properties E_1, E_2, ν_1, and ν_2 of individual constituent material are in functions of environment temperature T that can be expressed in the power-law function type of FGMs.

By defining the integrated expressions of $\bar{Q}_{i^s j^s}$ and $\bar{Q}_{i^* j^*}$ in the direction of z axis for the thick FGM cylindrical shells as follows,

$$(A_{i^s j^s}, B_{i^s j^s}, D_{i^s j^s}, E_{i^s j^s}, F_{i^s j^s}, H_{i^s j^s}) = \int_{-\frac{h^*}{2}}^{\frac{h^*}{2}} \bar{Q}_{i^s j^s} (1, z, z^2, z^3, z^4, z^6) dz \ , \ (i^s, j^s = 1,2,6)$$

$$(A_{i^* j^*}, B_{i^* j^*}, D_{i^* j^*}, E_{i^* j^*}, F_{i^* j^*}, H_{i^* j^*}) = \int_{-\frac{h^*}{2}}^{\frac{h^*}{2}} k_\alpha \bar{Q}_{i^* j^*} (1, z, z^2, z^3, z^4, z^5) dz \ , \ (i^*, j^* = 4,5) \tag{4}$$

in which k_α is the advanced shear correction coefficient can be represented in the rational expression form and functions of c_1, R_n, and T by Hong [23,24].

3. Numerical results and discussion

The thick FGM circular cylindrical shells with layers in the stacking sequence (0°/0°) are used to study the free vibration frequency with the effects of environment temperature and advanced varied shear correction coefficient, under four sides simply supported boundary condition (at $x = 0$ and $x = L$, $\partial u_0/\partial x = v_0 = w = \partial \phi_x/\partial x = \phi_\theta = 0$, at $\theta = 0$ and $\theta = 2\pi$, $u_0 = \partial v_0/\partial \theta = w = \phi_x = \partial \phi_\theta/\partial \theta = 0$) no thermal loads ($\Delta T = 0$), no in-plane distributed forces, and no external pressure load. The free vibration frequency (ω_{mn} with mode shape number in subscripts m and n) can be derived by simply assuming that $I_1 = I_3 = J_1 = 0$, $B_{ij} = E_{ij} = 0$, $A_{16} = A_{26} = 0$, $D_{16} = D_{26} = 0$, and $A_{45} = D_{45} = F_{45} = 0$, where $I_i = \sum_{k=1}^{N^*} \int_k^{k+1} \rho^{(k)} z^i dz$, ($i = 0,1,2,\cdots,6$), in which N^* is the total number of layers, $\rho^{(k)}$ is the density of kth ply, $J_i = I_i - c_1 I_{i+2}$, ($i = 1,4$), also define $K_2 = I_2 - 2c_1 I_4 + c_1^2 I_6$ under the following time sinusoidal displacement and shear rotations with amplitudes a_{mn}, b_{mn}, c_{mn}, d_{mn} and e_{mn}.

$$u_0 = a_{mn} \cos(m\pi x/L) \sin(n\pi\theta/R) \sin(\omega_{mn}t)$$

$$v_0 = b_{mn} \sin(m\pi x/L) \cos(n\pi\theta/R) \sin(\omega_{mn}t)$$

$$w = c_{mn} \sin(m\pi x/L) \sin(n\pi\theta/R) \sin(\omega_{mn}t) \tag{5}$$

$$\varphi_x = d_{mn} \cos(m\pi x/L) \sin(n\pi\theta/R) \sin(\omega_{mn}t)$$

$$\varphi_\theta = e_{mn} \sin(m\pi x/L) \cos(n\pi\theta/R) \sin(\omega_{mn}t)$$

where subscripts m is the number of axial half-waves and n is the number of circumferential waves. By substituting Eqs. (5) into dynamic equilibrium differential equations with TSDT of FGM circular cylindrical shells in terms of partial derivatives of displacements and shear rotations under free vibration (without the thermal loads and mechanical loads), the fully homogeneous equation can be obtained as follows:

$$\begin{bmatrix} s_{11} & s_{12} & s_{13} & s_{14} & s_{15} \\ s_{21} & s_{22} & s_{23} & s_{24} & s_{25} \\ s_{31} & s_{32} & s_{33} & s_{34} & s_{35} \\ s_{41} & s_{42} & s_{43} & s_{44} & s_{45} \\ s_{51} & s_{52} & s_{53} & s_{54} & s_{55} \end{bmatrix} \begin{Bmatrix} a_{mn} \\ b_{mn} \\ c_{mn} \\ d_{mn} \\ e_{mn} \end{Bmatrix} = \begin{Bmatrix} 0 \\ 0 \\ 0 \\ 0 \\ 0 \end{Bmatrix} \tag{6}$$

where

$$s_{11} = FH_{11} - \frac{I_0 \lambda_{mn}}{I_0}, \ \ s_{12} = FH_{12}, \ \ s_{13} = FH_{13} + \frac{c_1 I_3 \left(\frac{m\pi}{L}\right)\lambda_{mn}}{I_0}, \ \ s_{14} = FH_{14} - \frac{J_1 \lambda_{mn}}{I_0}, \ \ s_{15} = FH_{15},$$

$$s_{21} = FH_{12}, \ \ s_{22} = FH_{22} - \frac{I_0 \lambda_{mn}}{I_0}, \ \ s_{23} = FH_{23} + \frac{c_1 I_3 \left(\frac{n\pi}{R}\right)\lambda_{mn}}{I_0}, \ \ s_{24} = FH_{24}, \ \ s_{25} = FH_{25} - \frac{J_1 \lambda_{mn}}{I_0},$$

$$s_{31} = FH_{13} + \frac{c_1 I_3 \left(\frac{m\pi}{L}\right)\lambda_{mn}}{I_0}, \ \ s_{32} = FH_{23} + \frac{c_1 I_3 \left(\frac{n\pi}{R}\right)\lambda_{mn}}{I_0},$$

$$s_{33} = FH_{33} - [I_0 + c_1{}^2 I_6 \left(\frac{m\pi}{L}\right)^2 + c_1{}^2 I_6 \left(\frac{n\pi}{R}\right)^2]\lambda_{mn}/I_0,$$

$$s_{34} = FH_{34} + \frac{c_1 J_4 \left(\frac{m\pi}{L}\right)\lambda_{mn}}{I_0}, \ \ s_{35} = FH_{35} + \frac{c_1 J_4 \left(\frac{n\pi}{R}\right)\lambda_{mn}}{I_0},$$

$$s_{41} = FH_{14} - \frac{J_1 \lambda_{mn}}{I_0}, \ \ s_{42} = FH_{24}, \ \ s_{43} = FH_{34} + \frac{c_1 J_4 \left(\frac{m\pi}{L}\right)\lambda_{mn}}{I_0}, \ \ s_{44} = FH_{44} - \frac{K_2 \lambda_{mn}}{I_0}, \ \ s_{45} = FH_{45},$$

$$s_{51} = FH_{15}, \ \ s_{52} = FH_{25} - \frac{J_1 \lambda_{mn}}{I_0}, \ \ s_{53} = FH_{35} + \frac{c_1 J_4 \left(\frac{n\pi}{R}\right)\lambda_{mn}}{I_0}, \ \ s_{54} = FH_{45}, \ \ s_{55} = FH_{55} - \frac{K_2 \lambda_{mn}}{I_0},$$

$$\lambda_{mn} = I_0 \omega_{mn}{}^2, FH_{11} = A_{11}(m\pi/L)^2 + A_{66}(n\pi/R)^2, \ \ FH_{12} = (A_{12} + A_{66})(m\pi/L)(n\pi/R),$$

$$FH_{13} = -c_1 E_{11}(m\pi/L)^3 - (c_1 E_{12} + 2c_1 E_{66})(m\pi/L)(n\pi/R)^2,$$

$$FH_{14} = (B_{11} - c_1 E_{11})(m\pi/L)^2 + (B_{66} - c_1 E_{66})(n\pi/R)^2,$$

$$FH_{15} = (B_{12} + B_{66} - c_1 E_{12} - c_1 E_{66})(m\pi/L)(n\pi/R), \ \ FH_{22} = A_{66}(m\pi/L)^2 + A_{22}(n\pi/R)^2,$$

$$FH_{23} = -(c_1 E_{12} + 2c_1 E_{66})(m\pi/L)^2(n\pi/R) - c_1 E_{22}(n\pi/R)^3,$$

$$FH_{24} = (B_{12} + B_{66} - c_1 E_{12} - c_1 E_{66})(m\pi/L)(n\pi/R),$$

$$FH_{25} = (B_{66} - c_1 E_{66})(m\pi/L)^2 + (B_{22} - c_1 E_{22})(n\pi/R)^2, \text{ etc.}$$

$$A_{11} = \frac{h^*}{1-(\frac{\nu_1+\nu_2}{2})^2}\left(\frac{R_n E_1 + E_2}{R_n+1}\right), E_{11} = \frac{(h^*)^4(E_2 - E_1)}{1-(\frac{\nu_1+\nu_2}{2})^2}\left[\frac{1}{R_n+4} - \frac{3}{2(R_n+3)} + \frac{3}{4(R_n+2)} - \frac{1}{8(R_n+1)}\right],$$

$$F_{11} = \frac{(h^*)^5}{1-(\frac{\nu_1+\nu_2}{2})^2}\left\{(E_2 - E_1)\left[\frac{1}{R_n+5} - \frac{2}{R_n+4} + \frac{1}{R_n+3} - \frac{1}{2(R_n+2)} + \frac{1}{16(R_n+1)}\right] + \frac{E_1}{80}\right\},$$

$$H_{11} = \frac{(h^*)^7}{1-(\frac{\nu_1+\nu_2}{2})^2}\left\{(E_2 - E_1)\left[\frac{1}{R_n+7} - \frac{3}{R_n+6} + \frac{13}{4(R_n+5)} - \frac{2}{R_n+4} + \frac{13}{16(R_n+3)} - \frac{3}{16(R_n+2)} + \frac{1}{64(R_n+1)}\right] + \frac{E_1}{448}\right\},$$

$$H_{44} = \frac{k_\alpha (h^*)^6 (E_2 - E_1)}{2(1 + \frac{v_1 + v_2}{2})} \left[\frac{1}{R_n + 6} - \frac{5}{2(R_n + 5)} + \frac{2}{R_n + 4} - \frac{1}{R_n + 3} + \frac{5}{64(R_n + 2)} - \frac{1}{32(R_n + 1)} \right], \text{etc}$$

The determinant of the coefficient matrix in equation (6) vanishes for obtaining the non-trivial solution of amplitudes, the polynomial equation in the fifth-order of λ_{mn} can be obtained as follows, thus the ω_{mn} can be found.

$$A(1)\lambda_{mn}{}^5 + A(2)\lambda_{mn}{}^4 + A(3)\lambda_{mn}{}^3 + A(4)\lambda_{mn}{}^2 + A(5)\lambda_{mn} + A(6) = 0 \tag{7}$$

where

$$A(1) = \sum_{i=1}^{20} d_i h_i, \quad A(2) = \sum_{i=1}^{20}(d_i g_i + b_i h_i), \quad A(3) = \sum_{i=1}^{20}(d_i ff_i + b_i g_i + a_i h_i),$$

$$A(4) = \sum_{i=1}^{20}(d_i e_i + b_i ff_i + a_i g_i), \quad A(5) = \sum_{i=1}^{20}(b_i e_i + a_i ff_i), \quad A(6) = \sum_{i=1}^{20} a_i e_i$$

where

$$a_1 = FH_{11}FH_{12}, \; b_1 = -(FH_{11} + FH_{22})I_0, \; d_1 = I_0{}^2,$$

$$e_1 = FH_{33}FH_{44}FH_{55} + 2FH_{34}FH_{35}FH_{45} - FH_{35}{}^2 FH_{44} - FH_{34}{}^2 FH_{55} - FH_{33}FH_{45}{}^2,$$

$$ff_1 = -FH_{33}FH_{55}K_2 - FH_{44}FH_{55}SI_{06} - FH_{33}FH_{44}K_2 + FH_{33}K_2{}^2 + FH_{44}K_2 SI_{06} + 2FH_{34}FH_{45}c_1 J_4 n\pi/R + 2FH_{35}FH_{45}c_1 J_4 m\pi/L - 2FH_{35}FH_{44}c_1 J_4 n\pi/R + FH_{35}{}^2 K_2 - 2FH_{34}FH_{55}c_1 J_4 m\pi/L + FH_{34}{}^2 K_2 + FH_{45}{}^2 SI_{06},$$

$$g_1 = FH_{55}K_2 SI_{06} + 2FH_{45}c_1{}^2 J_4{}^2 (m\pi/L)(n\pi/R) - FH_{44}c_1{}^2 J_4{}^2 (n\pi/R)^2 + 2FH_{35}K_2 c_1 J_4 n\pi/R - FH_{55}c_1{}^2 J_4{}^2 (m\pi/L)^2 + 2FH_{34}K_2 c_1 J_4 m\pi/L,$$

$$h_1 = -K_2{}^2 SI_{06} + K_2 c_1{}^2 J_4{}^2 (n\pi/R)^2 + K_2 c_1{}^2 J_4{}^2 (m\pi/L)^2, \text{etc.}$$

$$a_{20} = -FH_{15}FH_{24}, \qquad b_{20} = 0, \qquad d_{20} = 0,$$

$$e_{20} = FH_{13}FH_{24}FH_{35} + FH_{15}FH_{23}FH_{34} + FH_{14}FH_{25}FH_{33} - FH_{15}FH_{24}FH_{33} - FH_{14}FH_{23}FH_{35} - FH_{13}FH_{25}FH_{34},$$

$$ff_{20} = -FH_{25}FH_{33}J_1 + FH_{23}FH_{35}J_1 + FH_{13}FH_{24}c_1 J_4 n\pi/R + FH_{24}FH_{35}c_1 I_3 m\pi/L - FH_{14}FH_{33}J_1 + FH_{15}FH_{23}c_1 J_4 m\pi/L + FH_{15}FH_{34}c_1 I_3 n\pi/R - FH_{25}FH_{34}c_1 I_3 m\pi/L + FH_{13}FH_{34}J_1 - FH_{14}FH_{35}c_1 I_3 n\pi/R - FH_{14}FH_{23}c_1 J_4 n\pi/R - FH_{13}FH_{25}c_1 J_4 m\pi/L - FH_{14}FH_{25}SI_{06} + FH_{15}FH_{24}SI_{06},$$

$$g_{20} = FH_{35}J_1 c_1 I_3 n\pi/R + FH_{23}J_1 c_1 J_4 n\pi/R + FH_{13}J_1 c_1 J_4 m\pi/L + FH_{34}J_1 c_1 I_3 m\pi/L + FH_{24}I_3 c_1{}^2 J_4 (m\pi/L)(n\pi/R) + FH_{15}I_3 c_1{}^2 J_4 (m\pi/L)(n\pi/R) - FH_{14}J_4 c_1{}^2 I_3 (n\pi/R)^2 - FH_{25}J_4 c_1{}^2 I_3 (m\pi/L)^2 + FH_{33}J_1{}^2 + FH_{25}J_1 SI_{06} + FH_{14}J_1 SI_{06}$$

$$h_{20} = I_3 J_4 c_1{}^2 J_1 (n\pi/R)^2 + I_3 J_4 c_1{}^2 J_1 (m\pi/L)^2 - J_1{}^2 SI_{06}$$

$$SI_{06} = I_0 + c_1{}^2 I_6 [(m\pi/L)^2 + (n\pi/R)^2]$$

Composited thick FGM SUS304/Si3N4 material is used to implement the numerical computation of vibration under environment temperature T. The FGM constituent material 1 at the inner position of shells is SUS304, and the FGM constituent material 2 at the outer position of shells is Si3N4 used for the free vibration frequency computations with the fully homogeneous equation. The advanced varied values of k_α are usually functions of c_1, R_n, and T in the thick FGM circular cylindrical shells ($B_{ij} \neq 0$). For $L/R = 1$, $h_1 = h_2$, $h^* = 1.2$ mm, advanced calculated values of nonlinear k_α are increasing with R_n (values from 0.1 to 10). Thus advanced values of k_α are used for frequency calculations of the free vibration including the effects of nonlinear coefficient c_1 term.

Table 1a. f^* for SUS304/Si3N4

L/h^*	R_n	c_1 (1/mm²)	f^*				
			Present solution, $h^* = 1.2$ mm, advanced nonlinear k_α				
			$T = 1K$	$T = 100K$	$T = 300K$	$T = 600K$	$T = 1000K$
5	0.5	0.925925	0.502130	0.570210	0.745849	0.773258	0.549213
		0	0.590006	0.643852	0.738035	0.792276	0.693156
	1	0.925925	0.542049	0.635356	1.088972	1.061970	0.583895
		0	0.584454	0.639541	0.735365	0.789534	0.682771
	2	0.925925	0.720395	0.147456	1.749742	1.857381	0.643730
		0	0.601933	0.657577	0.754101	0.809998	0.705449
	10	0.925925	0.439585	0.432449	1.912712	2.034272	0.575911
		0	0.714064	0.765051	0.856587	0.920757	0.874146
8	0.5	0.925925	0.384405	0.432271	0.549680	0.572973	0.417923
		0	0.275399	0.300743	0.345240	0.371763	0.325808
	1	0.925925	0.412331	0.475557	0.734396	0.732705	0.444527
		0	0.270439	0.296031	0.341274	0.367443	0.316992
	2	0.925925	0.520187	0.256231	0.966141	1.024323	0.492228
		0	0.278029	0.303717	0.349439	0.376290	0.326585
	10	0.925925	6.133640	0.966218	1.064178	1.131785	1.103627
		0	0.333380	0.359943	0.403599	0.435239	0.415926
10	0.5	0.925925	0.444867	0.489384	0.591412	0.618544	0.501530
		0	0.193089	0.209523	0.242446	0.259834	0.229385
	1	0.925925	0.468606	0.523140	32.68439	0.734637	0.529650
		0	0.184350	0.206358	0.239394	0.257086	0.215634
	2	0.925925	2.502079	0.307402	0.638958	0.678791	0.569559
		0	0.186246	0.211788	0.244852	0.263350	0.215261
	10	0.925925	0.481267	0.507236	0.551137	0.587717	0.588011
		0	0.236454	0.250857	0.283276	0.304129	0.291925

Non-dimensional frequency parameter $f^* = 4\pi\omega_{11}R\sqrt{I_2/A_{11}}$ values under the effects of $c_1 = 0.925925/\text{mm}^2$ and $c_1 = 0/\text{mm}^2$ for $L/h^* = 5, 8$, and 10 are shown in Table 1a, where ω_{11} is the fundamental first natural frequency (subscripts $m = n = 1$). For SUS304/Si3N4 thick circular cylindrical shells under free vibration with $h^* = 1.2$ mm, the h^* values are in the values not greater than 32.68439 under $T = 1K, 100K, 300K, 600K$, and $1000K$ with advanced nonlinear varied k_α and c_1 effects. Thus the f^* values are in functions of five parameters L/h^*, R_n, c_1, T, and k_α. The other non-dimensional frequency parameter $\Omega = (\omega_{11}L^2/h^*)\sqrt{\rho_1/E_1}$ values under the effects of $c_1 = 0.925925/\text{mm}^2$ and $c_1 = 0/\text{mm}^2$ for $L/h^* = 5, 8$, and 10 are shown in Table 1b, ρ_1 is the density of FGM material 1, for SUS304/Si3N4 thick circular cylindrical shells under free vibration with $h^* = 1.2$ mm, the Ω values are in the values not greater than 109.2509 under $T = 1K, 100K, 300K, 600K$, and $1000K$ with advanced nonlinear varied k_α and c_1 effects. Thus the Ω values are also in functions of five parameters L/h^*, R_n, c_1, T, and k_α. The natural frequencies calculated from the polynomial Eq. (7) with the determinant of fully homogeneous matrix eq.(6),

there are containing the dominant parameters c_1 and k_α for the present advanced TSDT study. Some natural frequencies in the published and referred paper with classical theory studies are given for comparisons. It is interesting to compare the present vibration values of the frequency with some authors' work as shown in Tables 1c-d. The values of f^* vs. h^* for SUS304/Si3N4 under $L/h^* = 10$ and $T = 300K$ with advanced nonlinear varied k_α and c_1 effects are shown in Table 1c. The compared value $f^* = 8.121246$ at $c_1 = 0.252047/mm^2$, $h^* = 2.3$ mm, $R_n = 0.5$ is greater than that $f^* = 8.0$ at $n = 13$ with silicon nitride–nickel under classical shell theory (CST), no external pressure ($Ke = 0$) presented by Sepiani et al. [22]. The compared f^* difference of 1.5% at $R_n = 0.5$ is due to the dominant parameters R_n, c_1, and k_α effects included in the present advanced TSDT study. The values of Ω vs. h^* for SUS304/Si3N4 under $L/h^* = 10$ and T=700K with advanced nonlinear varied k_α and c_1 effects are shown in Table 1d. The compared value $\Omega = 1.719431$ at $c_1 = 1.101928/mm^2$, $h^* = 1.1$ mm, $R_n = 1$ is close to $\Omega = 1.71137$ with the material variation type A, three layers thickness ratio 1-8-1, the L directional radius of curvature is ∞, $L/h^* = 10$, $R_n = 0.5$ for the FGM sandwich shell presented by Chen et al. [25]. The compared Ω difference of 6.4% at $R_n = 0.5$ is due to the dominant parameters c_1 and k_α effects included in the present advanced TSDT study.

Table 1b. Ω for SUS304/Si3N4

L/h^*	R_n	c_1 (1/mm²)	Ω				
			Present solution, $h^* = 1.2$ mm, advanced nonlinear k_α				
			$T = 1K$	$T = 100K$	$T = 300K$	$T = 600K$	$T = 1000K$
5	0.5	0.925925	0.913275	1.013033	1.288651	1.341320	1.068076
		0	1.073105	1.143866	1.275150	1.374310	1.348008
	1	0.925925	0.944602	1.086094	1.820001	1.781280	1.077132
		0	1.018498	1.093247	1.229017	1.324313	1.259533
	2	0.925925	1.198026	0.241754	2.822099	3.005259	1.119442
		0	1.001023	1.078098	1.216264	1.310585	1.226770
	10	0.925925	0.676893	0.662559	2.914729	3.107570	0.905644
		0	1.099547	1.172142	1.305329	1.406556	1.374629
8	0.5	0.925925	1.118652	1.228756	1.519547	1.590239	1.300403
		0	0.801435	0.854879	0.954389	1.031797	1.013780
	1	0.925925	1.149677	1.300685	1.963837	1.966387	1.312058
		0	0.754050	0.809668	0.912595	0.986122	0.935628
	2	0.925925	1.384125	0.672145	2.493210	2.651783	1.369569
		0	0.739785	0.796712	0.901757	0.974145	0.908687
	10	0.925925	15.111748	2.368561	2.594676	2.766279	2.776796
		0	0.821366	0.882354	0.984053	1.063799	1.046497
10	0.5	0.925925	1.618253	1.738877	2.043641	2.145896	1.950690
		0	0.702381	0.744476	0.837780	0.901436	0.892191
	1	0.925925	1.633234	1.788537	109.2509	2.464468	1.954131
		0	0.642515	0.705509	0.800200	0.862442	0.795578
	2	0.925925	108.10273	1.007971	2.061109	2.196582	1.980920
		0	0.619460	0.694453	0.789826	0.852205	0.748676
	10	0.925925	1.482151	1.554282	1.679727	1.795602	1.849342
		0	0.728204	0.768680	0.863353	0.929181	0.918128

Table 1c. Comparison of frequency f^* for SUS304/Si₃N₄ and silicon nitride–nickel

c_1 (1/mm²)	h^* (mm)	Present method, $L/h^* = 10, T = 300K$, advanced nonlinear k_α, for SUS304/Si₃N₄			Sepiani et al. 2010 [22], for silicon nitride–nickel, $n = 13$
		$R_n = 0.5$	$R_n = 1$	$R_n = 2$	
6.584362	0.45	0.085005	0.101168	0.077682	-
0.925925	1.2	0.591412	32.68439	0.638958	-
0.333333	2	5.089255	5.388204	5.345398	-
0.275482	2.2	7.027582	7.420739	7.400630	-
0.252047	2.3	8.121246	8.565044	8.558597	8.0
0.231481	2.4	9.299983	9.798618	9.807841	-
0.000003	600	18032.99	18729.97	19240.79	-

Table 1c. Comparison of frequency Ω for SUS304/Si₃N₄

c_1 (1/mm²)	h^* (mm)	Present method, $L/h^* = 10, T = 700K$, advanced nonlinear k_α			Chen et al. 2017 [25], Type A, 1-8-1, $R_n = 0.5$
		$R_n = 0.5$	$R_n = 1$	$R_n = 2$	
6.584362	0.45	0.811649	0.837942	0.674542	-
1.333333	1.0	1.338406	1.450429	2.509230	-
1.101928	1.1	1.601360	1.719431	2.364609	1.71137
0.925925	1.2	2.069517	2.187293	2.099298	-
0.000014	300	33198.62	33146.66	33434.83	-
0.000003	600	133.3191	133.4515	132.7114	-
0.000001	900	211.7611	211.8620	211.3022	-

Natural frequencies ω_{mn} (1/s) of free vibration according to mode shape numbers m and n at the subscripts for the SUS304/Si3N4 FGM thick circular cylindrical shells are calculated. For the values of fundamental ω_{11} vs. R_n with $h^* = 1.2 mm$, advanced nonlinear varied k_α and $c_1 = 0.925925/mm^2$ for $L/h^* = 5$ and 10 under $T = 1K, 100K, 300K, 600K$ and $1000K$ are shown in Table 2. The ω_{11} values at $c_1 = 0.925925/mm^2$ and advanced nonlinear k_α are in functions of three parameters L/h^*, R_n, and T. For the values of natural frequency ω_{mn} vs. subscripts $m, n = 1, 2, \ldots, 9$ with $R_n = 0.5$, $T = 300K$, $h^* = 1.2$ mm under advanced nonlinear varied k_α and $c_1 = 0.925925/mm^2$ for $L/h^* = 5$ and 10 can also be calculated. Typically, the advanced nonlinear varied k_α values for $T = 300K$ are listed in the Table 3. The k_α values at $c_1 \neq 0$, $c_1 = 0$ and $T = 300K$ are in nonlinear function of the parameter R_n. Also the nonlinear values of k_α are independent of $h *$ for the thick FGM circular cylindrical shells. Some usual abbreviations and denotations have been added in Nomenclature for convenient reading.

Natural frequency ω_{mn} (subscripts $m = 1, n = 1\ to\ 9$) values vs. R_n and T of free vibration for the SUS304/Si3N4 FGM thick circular cylindrical shells are calculated. Fig. 2 shows the values of ω_{1n} vs. R_n in FGM circular cylindrical shells for thick $L/h^* = 5, 10$ respectively, with the effects of advanced nonlinear varied k_α and $c_1 = 0.925925/mm^2$ under $T = 300K$. Generally the values of ω_{1n} are little decreasing with

subscript values of n from 1 to 6 then great increasing with subscript values of n from 7 to 8 for $L/h^* = 5$, $R_n = 0.5$, and 10. The greatest value $\omega_{18} = 0.006449/s$ is found for $L/h^* = 5$ and $R_n = 1$. The values of ω_{1n} are decreasing with subscript values of n from 1 to 9 for $L/h^* = 10$, $R_n = 1$. The values of ω_{1n} are great increasing with subscript values of n from 1 to 2 and then decreasing with subscript values of n from 3 to 9 for $L/h^* = 5$, $R_n = 0.5$ and 10. The greatest value $\omega_{11} = 0.007780/s$ is found for $L/h^* = 10$. The values of ω_{1n} with subscript values of n from 4 to 9 also do not be affected by R_n for $L/h^* = 10$. The ω_{1n} values at $c_1 = 0.925925/mm^2$, $T = 300K$ and advanced nonlinear k_α are in functions of parameters L/h^* and R_n.

Table 2. Fundamental natural frequency ω_{11} for advanced nonlinear k_α, c_1, $h^* = 1.2$ mm

L/h^*	R_n	ω_{11}				
		$T = 1K$	$T = 100K$	$T = 300K$	$T = 600K$	$T = 1000K$
5	0.5	0.000255	0.000287	0.000367	0.000366	0.000242
	1	0.000264	0.000307	0.000518	0.000486	0.000244
	2	0.000335	0.000068	0.000803	0.000820	0.000253
	10	0.000189	0.000187	0.000830	0.000848	0.000205
10	0.5	0.000113	0.000123	0.000145	0.000146	0.000110
	1	0.000114	0.000126	0.007780	0.000168	0.000110
	2	0.007573	0.000071	0.000146	0.000149	0.000112
	10	0.000103	0.000110	0.000119	0.000122	0.000104

Table 3. Advanced nonlinear k_α, c_1 and R_n under $T = 300K$

c_1 (1/mm^2)	h^* (mm)	k_α						
		$R_n = 0.1$	$R_n = 0.2$	$R_n = 0.5$	$R_n = 1$	$R_n = 2$	$R_n = 5$	$R_n = 10$
92.592598	0.12	-0.821563	-0.861922	-1.181502	-4.392330	1.474843	0.583927	0.463616
0.925925	1.2	-0.821565	-0.861923	-1.181503	-4.392341	1.474844	0.583927	0.463617
0.231481	2.4	-0.821565	-0.861923	-1.181503	-4.392341	1.474844	0.583927	0.463617
0.037037	6	-0.821564	-0.861924	-1.181502	-4.392332	1.474843	0.583927	0.463617
0.009259	12	-0.821564	-0.861924	-1.181503	-4.392332	1.474843	0.583927	0.463617
0	0.12	0.898426	0.956500	1.087890	1.195721	1.226106	1.121959	1.019033
0	1.2	0.898426	0.956498	1.087891	1.195721	1.226106	1.121959	1.019034
0	2.4	0.898426	0.956498	1.087891	1.195721	1.226106	1.121959	1.019034
0	6	0.898425	0.956496	1.087891	1.195721	1.226106	1.121958	1.019033
0	12	0.898426	0.956495	1.087891	1.195721	1.226106	1.121958	1.019033

Fig. 3 shows the values of ω_{1n} vs. T in FGM circular cylindrical shells for thick $L/h^* = 5$ and 10 respectively, under the effects of advanced nonlinear varied k_α, $c_1 = 0.925925/\text{mm}^2$ and $R_n = 0.5$. Generally the values of ω_{1n} are little decreasing with subscript values of n from 1 to 6 then great increasing with next subscript values of n for $L/h^* = 5$, $T = 300K, 600K$ and $1000K$. The greatest value of $\omega_{17} = 0.007372/s$ is found for $L/h^* = 5$, $T = 1000K$. The values of ω_{1n} can't stand for higher temperature $T = 1000K$ for $L/h^* = 5$. The values of ω_{1n} are great increasing with subscript values of n from 1 to 2 and then decreasing with subscript values of n from 3 to 9 for $L/h^* = 10$, $T = 300K, 600K$ and $1000K$. The values of ω_{1n} are almost the same for $T = 300K$ and $600K$, but in greater values than that in the $T = 1000K$. The greatest value of $\omega_{12} = 0.005455/s$ is found for $L/h^* = 10$, $T = 600K$. The values of ω_{1n} can stand for higher temperature $T = 1000K$ for $L/h^* = 10$. The ω_{1n} values at $c_1 = 0.925925/\text{mm}^2$, $R_n = 0.5$ and advanced nonlinear k_α are in functions of parameters L/h^* and T.
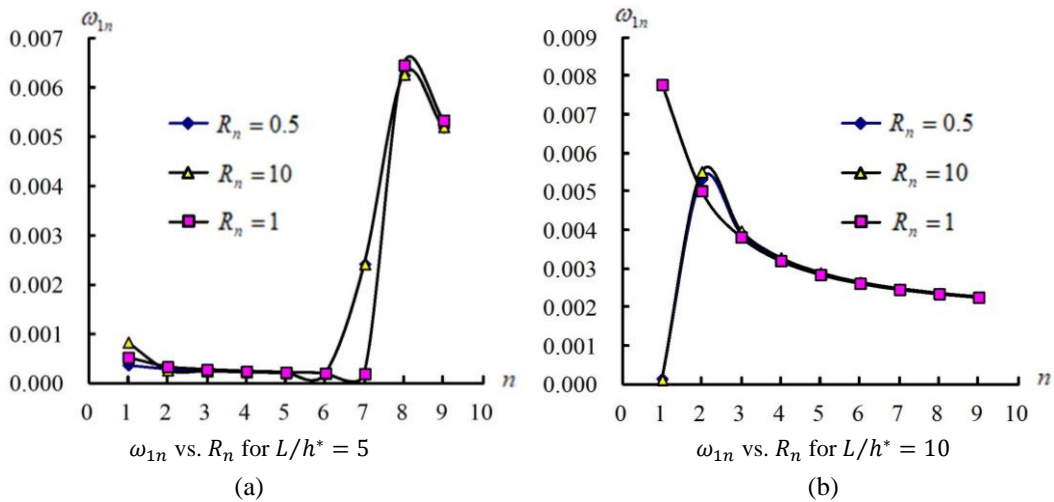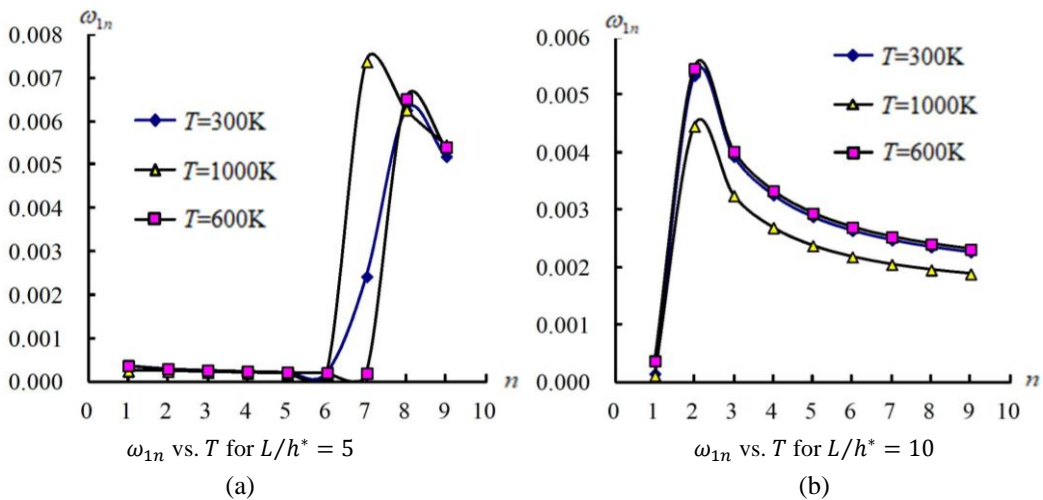

ω_{1n} vs. R_n for $L/h^* = 5$

(a)

ω_{1n} vs. R_n for $L/h^* = 10$

(b)

Fig. 2. ω_{1n} vs. R_n for $L/h^* = 5$ and 10

ω_{1n} vs. T for $L/h^* = 5$

(a)

ω_{1n} vs. T for $L/h^* = 10$

(b)

Fig. 3. ω_{1n} vs. T for $L/h^* = 5$ and 10

f^{**} vs. n for $m = 1 - 3$, $L/h^* = 5$ with advanced nonlinear k_α, $c_1 = 0.333333/mm^2$

(a)

f^{**} vs. n for $m = 1 - 3$, $L/h^* = 5$ with linear varied k_α, $c_1 = 0/mm^2$

(b)

f^{**} vs. n for $m = 1 - 3$, $L/h^* = 5$ with constant nonlinear $k_\alpha = 5/6$, $c_1 = 0.333333/mm^2$

(c)

f^{**} vs. n for $m = 1 - 3$, $L/h^* = 5$ with constant $k_\alpha = 5/6$, $c_1 = 0/mm^2$
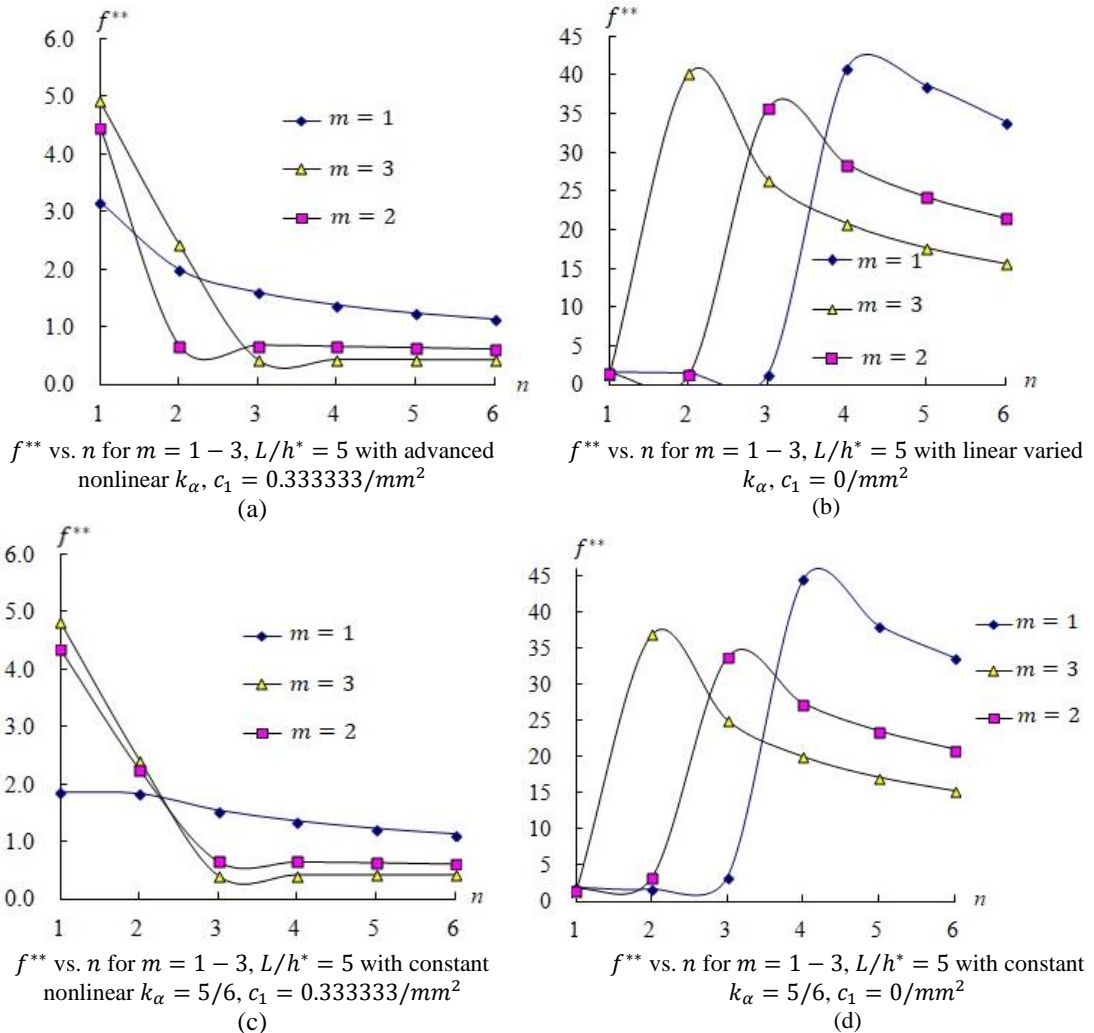
(d)

Fig. 4. f^{**} vs. n for $m = 1 - 3$, $L/h^* = 5$ with varied and constant k_α

Compared values of $f^{**} = 4\pi\omega_{mn}R\sqrt{I_2/A_{11}}$ vs. subscript values $n = 1 - 6$ for $m = 1, 2, 3$ with $R_n = 0.5$, $h^* = 2$ mm, $T = 300K$ are shown in Fig. 4 for the SUS304/Si3N4 FGM thick circular cylindrical shells, $L/h^* = 5$, respectively by considering advanced nonlinear k_α, $c_1 = 0.333333/mm^2$, linear varied k_α, $c_1 = 0/mm^2$ and constant $k_\alpha = 5/6$. The presented numerical frequencies f^{**} are decreasing firstly vs. circumferential nodes $n = 1 - 6$ in the axial nodes $m = 1, 2, 3$ of FGM cylindrical shells in both Fig. 4a and Fig. 4c. In Fig. 4a, $f^{**} = 3.151624$ is obtained at $m = n = 1$ with advanced nonlinear k_α, $c_1 = 0.333333/mm^2$. The compared f^{**} values under advanced nonlinear k_α, $c_1 = 0.333333/mm^2$ are in decreasing functions of mode shapes m and n. In Fig. 4c, $f^{**} = 1.851984$ is obtained at $m = n = 1$ with constant $k_\alpha = 5/6$, $c_1 = 0.333333/mm^2$. The compared f^{**} values under constant $k_\alpha = 5/6$, $c_1 = 0.333333/mm^2$ are in decreasing functions of mode shapes m and n. The presented numerical frequencies f^{**} are increasing to around 45 firstly and then decreasing vs. $n = 1 - 6$ in the $m = 1, 2, 3$ of FGM cylindrical shells in both Fig. 4b and Fig. 4d. In Fig. 4b, $f^{**} = 1.655910$ is obtained at $m = n = 1$ with varied k_α, $c_1 = 0/mm^2$. The compared f^{**} values under linear varied k_α and $c_1 = 0/mm^2$ are in increasing then decreasing functions of mode shapes m and n. In Fig. 4d, $f^{**} = 1.843023$ is obtained at $m = n = 1$

with constant $k_\alpha = 5/6$, $c_1 = 0/mm^2$. The compared f^{**} values under constant $k_\alpha = 5/6$, $c_1 = 0/mm^2$ are in increasing then decreasing functions of mode shapes m and n. There are great effects of nonlinear coefficient term c_1 and k_α on the value of frequencies by using the approaching of fully homogeneous equations. In the linear case $c_1 = 0/mm^2$, the values of f^{**} are overestimated. It is quite reasonable to consider the effect of nonlinear varied values k_α and c_1 on the advanced calculation of natural frequencies by using the approaching of fully homogeneous equations.

4. Conclusion

Natural frequency and non-dimensional frequency parameters are calculated and obtained by using the fully homogeneous equation with the polynomial equation in the fifth-order of λ_{mn} in the free vibration of thick FGM circular cylindrical shells. There are four effects of nonlinear coefficient term c_1, advanced nonlinear shear correction coefficient, power-law exponent parameter, and environment temperature considered and investigated on the natural frequencies. The values of ω_{1n} can't stand for higher temperature $T = 1000K$ for $L/h^* = 5$, but the values can stand for higher temperature $T = 1000K$ for $L/h^* = 10$.

Nomenclature

CST	Classical shell theory
FGM	Functionally graded material
FGMs	Functionally graded materials
FSDT	First-order shear deformation theory
TSDT	Third-order shear deformation theory
HSDT	Higher-order shear deformation theory
SUS304	Stainless steel
Si3N4	Silicon nitride
k_α	Shear correction coefficient of thick FGM cylindrical shells
$c_1 = 4/(3h^{*2})$	Nonlinear coefficient term of TSDT
$\Delta T = 0$	No thermal loads
T	Environment temperature
L	Length of FGM cylindrical shells
h^*	Thickness of FGM cylindrical shells
R	The middle-surface radius of FGM cylindrical shells
R_n	FGM power-law exponent parameter
ω_{mn}	The natural frequency with subscripts m and n mode shape
$f^* = 4\pi\omega_{11}R\sqrt{I_2/A_{11}}$	Non-dimensional frequency parameter 1
$\Omega = (\omega_{11}L^2/h^*)\sqrt{\rho_1/E_1}$	Non-dimensional frequency parameter 2
$f^{**} = 4\pi\omega_{mn}R\sqrt{I_2/A_{11}}$	Non-dimensional frequency parameter 1 vs. M and n

Conflict of interests

The author(s) declared no potential conflicts of interest with respect to the research, authorship, and/or publication of this article.

Funding

Data availability statement

Data generated during the current study are available from the corresponding author upon reasonable request.

References

[1]   Birman V, Bert CW (2002) On the choice of shear correction factor in sandwich structures. Journal of Sandwich Structures and Materials 4(1):83–95.

[2]   Okumus F (2004) An analysis of shear correction factors in a thermoplastic composite cantilever beam. Iranian Journal of Science & Technology, Transaction B 28(B4):501-504.

[3]   Daouadji TH, Tounsi A, Bedia EAA (2013) A new higher order shear deformation model for static behavior of functionally graded plates. Advances in Applied Mathematics and Mechanics 5:351–364.

[4]   Xiang S, Kang GW, Liu YQ (2014) A nth-order shear deformation theory for natural frequency of the functionally graded plates on elastic foundations. Composite Structures 111:224–231.

[5]   Lim TC (2016) Improved shear correction factors for deflection of simply supported very thick rectangular auxetic plates. International Journal of Mechanical and Materials Engineering 11:13.

[6]   Bouhlali M, Chikh A, Bouremana M, Kaci A, Bourada F, Belakhdar K, Tounsi A (2019) Nonlinear thermoelastic analysis of FGM thick plates. Coupled Systems Mechanics 8(5):439–457.

[7]   Ghamkhar M, Naeem MN, Imran M, Kamran M, Soutis C (2019) Vibration frequency analysis of three-layered cylinder-shaped shell with effect of FGM central layer thickness. Scientific Reports 9:1566.

[8]   Nguyen HN, Hong TT, Vinh PV, Quang ND, Thom DV (2019) A refined simple first-order shear deformation theory for static bending and free vibration analysis of advanced composite plates. Materials 12(15):2385.

[9]   Ganczarski A, Szubartowski D (2020) Problems of thick functionally graded material structures under thermomechanical loadings. Publisher: Springer International Publishing. In book: Advances in Mechanics of High-Temperature Materials (pp.57-78)

[10] Vuong PM, Duc ND (2020) Nonlinear vibration of FGM moderately thick toroidal shell segment within the framework of Reddy's third order-shear deformation shell theory. International Journal of Mechanics and Materials in Design 16(5):245–264.

[11] Yaylaci M, Öner E, Adıyaman G, Öztürk Ş, Yaylaci EU, Birinci A (2023) Analyzing of continuous and discontinuous contact problems of a functionally graded layer: theory of elasticity and finite element method. Mechanics Based Design of Structures and Machines, An International Journal. published online:09 Oct 2023.

[12] Adiyaman G, Oner E, Yaylaci M, Birinci A (2023) The contact problem of a functionally graded layer under the effect of gravity. Journal of Applied Mathematics and Mechanics 103(11):e202200560.

[13] Yaylaci M, Yaylaci EU, Ozdemir ME, Ozturk Ş, Sesli H (2023) Vibration and buckling analyses of FGM beam with edge crack: Finite element and multilayer perceptron methods. Steel and Composite Structures 46(4):565–575.

[14] Adiyaman G, Öner E, Yaylaci M, Birinci A (2023) A study on the contact problem of a layer consisting of functionally graded material (FGM) in the presence of body force. Journal of Mechanics of Materials and Structures 18(1):125–141.

[15] Turan M, Yaylaci EU, Yaylaci M (2023) Free vibration and buckling of functionally graded porous beams using analytical, finite element, and artificial neural network methods. Archive of Applied Mechanics 93(6):1351–1372.

[16] Hong CC (2020) Free vibration frequency of thick FGM spherical shells with simply homogeneous equation by using TSDT. Journal of the Brazilian Society of Mechanical Sciences and Engineering 42(159):1–15.

[17] Hong CC (2020) Free vibration frequency of thick FGM circular cylindrical shells with simply homogeneous equation by using TSDT. Advance in Technology Innovation 5(2):84–97.

[18] Hong CC (2017) Effects of varied shear correction on the thermal vibration of functionally-graded material shells in unsteady supersonic flow. Aerospace 4(1):1–15.

[19] Hong CC (2014) Thermal vibration of magnetostrictive functionally graded material shells by considering the varied effects of shear correction coefficient. International Journal of Mechanical Sciences 85:20–29.

[20] Lee SJ, Reddy JN, Rostam-Abadi F (2004) Transient analysis of laminated composite plates with embedded smart-material layers. Finite Elements in Analysis and Design 40(5-6):463–483.

[21] Whitney JM (1987) Structural Analysis of Laminated Anisotropic Plates. Technomic Publishing Company, Inc. Lancaster: Pennsylvania, USA.

[22] Sepiani HA, Rastgoo A, Ebrahimi F, Arani AG (2010) Vibration and buckling analysis of two-layered functionally graded cylindrical shell considering the effects of transverse shear and rotary inertia. Materials and Design 31(3):1063–1069.

[23] Hong CC (2022) Advanced dynamic thermal vibration of laminated FGM plates with simply homogeneous equation by using TSDT and nonlinear varied shear coefficient. Applied Sciences 12(22):11776.

[24] Hong CC (2022) Advanced frequency analysis of thick FGM plates using third-order shear deformation theory with a nonlinear shear correction coefficient. Journal of Structural Engineering & Applied Mechanics 5(3):143–160.

[25] Chen H, Wang A, Hao Y, Zhang W (2017) Free vibration of FGM sandwich doubly-curved shallow shell based on a new shear deformation theory with stretching effects. Composite Structures 179:50–60.